Ca2+ Sparks Triggered by Patch Depolarization in Rat Heart Cells

Stephen R. Shorofsky, Leighton Izu, Withrow Gil Wier and C. William Balke

Circ. Res. 1998;82;424-429
Circulation Research is published by the American Heart Association. 7272 Greenville Avenue, Dallas, TX 72514
 Print ISSN: 0009-7330. Online ISSN: 1524-4571

Ca^{2+} Sparks Triggered by Patch Depolarization in Rat Heart Cells

Stephen R. Shorofsky, Leighton Izu, Withrow Gil Wier, C. William Balke

Abstract—The goal of this study was to examine the relationship between Ca^{2+} entry through L-type Ca^{2+} channels and local $[Ca^{2+}]_i$ transients (Ca^{2+} sparks) in single rat cardiac ventricular cells. L-type Ca^{2+} channels were activated by depolarization of cell-attached membrane patches, and $[Ca^{2+}]_i$ was measured simultaneously as fluo 3 fluorescence using laser scanning confocal microscopy. Patch depolarization with Ca^{2+} as the charge carrier (10 or 110 mmol · L^{-1}) significantly increased the probability of the occurrence of Ca^{2+} sparks (Ca^{2+} spark rate) only in the volume of cytoplasm located immediately beneath the membrane patch (basal Ca^{2+} spark rate, 119 Ca^{2+} sparks · $cell^{-1}$ · s^{-1}; patch depolarization Ca^{2+} spark rate, 610 Ca^{2+} sparks · $cell^{-1}$ · s^{-1}; $P<.005$). With Ba^{2+} in the pipette solution (10 mmol · L^{-1}), patch depolarization was not associated with an increased Ca^{2+} spark rate at the position of the pipette or at any other sites distant from the pipette. Therefore, Ca^{2+} entry and not voltage per se was a necessary event for the occurrence of Ca^{2+} sparks. Under identical experimental conditions, patch depolarization experiments opened single L-type Ca^{2+} channels with a single-channel conductance of 19 pS with Ba^{2+} as the charge carrier. Although single-channel openings could not be resolved when Ca^{2+} was the charge carrier, ensemble averages yielded an inward current of up to 0.75 pA. The results suggest that voltage-activated Ca^{2+} entry through one or a small number of L type Ca^{2+} channels triggers the release of Ca^{2+} only from the sarcoplasmic reticulum in direct proximity to those L-type Ca^{2+} channels. The relatively low probability of triggering Ca^{2+} sparks may have resulted from some alteration of excitation-contraction coupling associated with the technique of the cell-attached patch clamp. **(*Circ Res*. 1998;82:424-429.)**

Key Words: heart ■ excitation-contraction coupling ■ Ca^{2+} spark ■ single L-type Ca^{2+} channel

A key unresolved issue in excitation-contraction coupling in heart is how the release of Ca^{2+} from the sarcoplasmic reticulum (SR) is prevented from triggering the uncontrolled regenerative release of additional Ca^{2+} from the SR. To solve this problem, the local control hypothesis[1–3] proposes that the transient elevation in $[Ca^{2+}]_i$ that triggers SR Ca^{2+} release is established locally in a restricted space (microdomain) between the sarcolemmal L-type Ca^{2+} channel and one or a small cluster of SR Ca^{2+} release channels located in the adjacent junctional SR. An additional feature of this hypothesis is that SR Ca^{2+} release does not trigger the further release of Ca^{2+} from nearby SR Ca^{2+} release channel(s). The experimental evidence supporting the local control hypothesis includes (1) the observation of spatially localized transient elevations in $[Ca^{2+}]_i$ visualized as Ca^{2+} sparks in single cardiac cells[4–7] and in intact cardiac muscle,[8] (2) the localization of Ca^{2+} sparks to the junction of the transverse tubule and the junctional SR,[9,10] where L-type Ca^{2+} channels and ryanodine receptors colocalize,[11] (3) the observation that the probability of evoking a Ca^{2+} spark has a voltage and time dependence similar to that of single L-type Ca^{2+} channels,[7] and (4) the ability of a single L-type Ca^{2+} channel to activate a Ca^{2+} spark as inferred from the voltage dependence of Ca^{2+} sparks at the foot of the activation curve for L-type Ca^{2+} current.[6,12] Although these results demonstrated a correspondence between the occurrence of Ca^{2+} sparks and whole-cell L-type Ca^{2+} current, it is difficult to make a direct association between Ca^{2+} sparks and local Ca^{2+} entry because individual L-type Ca^{2+} channels opened at unknown and random locations throughout the sarcolemma and transverse tubule membranes of the whole cell. In this study, we demonstrate that Ca^{2+} entry through one or a small number of L-type Ca^{2+} channels triggers Ca^{2+} release only from the SR in direct proximity to those channels.

Materials and Methods

Cell Preparation, Solutions, and Recording Conditions

Two-month-old Sprague-Dawley rats (200 to 300 g) were anesthetized with sodium pentobarbital (170 mg/kg IP). The hearts were removed from the animals via midline thoracotomy, and single ventricular cells were obtained by a standard enzymatic dispersion technique described in detail previously.[7] The cells were loaded with the Ca^{2+} indicator fluo 3 (Molecular Probes) by incubating the cells for 30 minutes at 25°C in control physiological salt–containing solutions to which fluo 3-AM (10 μmol/L) had been added. The

Received July 16, 1997; accepted December 12, 1997.

From the Departments of Medicine (S.R.S., L.I., W.G.W., C.W.B.) and Physiology (W.G.W., C.W.B.), University of Maryland School of Medicine, Baltimore, Md.

Reprint requests to C. William Balke, MD, University of Maryland School of Medicine, Department of Physiology, Room 544, Howard Hall, 665 W Redwood St, Baltimore, MD 21201.

E-mail bbalk001@umaryland.edu

external solution was composed of (mmol/L) NaCl 140, dextrose 10, HEPES 10, $MgCl_2$ 1, and $CaCl_2$ 0.5, pH adjusted to 7.3 with NaOH. The electrode-filling solution was composed of (mmol/L) either (1) $CaCl_2$ 110, HEPES 10, and tetraethylammonium (TEA)-Cl 30 or (2) TEA-Cl 130, HEPES 10, and either $CaCl_2$ 10 or $BaCl_2$ 10, pH adjusted to 7.3 with TEA-OH. In all experiments, the pipette solution included isoproterenol (1 μmol/L) to enhance the open probability of L-type Ca^{2+} channels, Bay K 8644 (10 μmol/L) to prolong the open time duration of L-type Ca^{2+} channels, and tetrodotoxin (20 μmol/L) to block Na^+ channels. All experiments were performed using standard electrophysiological methods with stable cell-attached membrane patches at room temperature (21°C to 23°C). In experiments in which Ca^{2+} sparks were recorded, the electrical resistance of the gigaseal was >4 to 5 GΩ. In experiments in which ensemble-averaged Ca^{2+} currents and single Ba^{2+} currents were recorded, the electrical resistance of the gigaseal was >10 GΩ. The ensemble-averaged L-type Ca^{2+} currents were filtered at 500 Hz, and the single Ba^{2+} currents were filtered at 1 kHz (Fig 4). The membrane patch was held at resting potential for 500 ms and subsequently depolarized for an additional 500 ms. Since the average resting potential of cells obtained by these methods was -78 ± 11 mV (n=16, data not shown), the membrane patch was depolarized by 80 mV to bring the potential of the membrane patch to ≈0 mV. Current was digitized at 2 kHz with 12-bit resolution.

Animals used in the present study were maintained in accordance with the guidelines of the Institutional Animal Care and Use Committee of the University of Maryland School of Medicine and the *Guide for the Care and Use of Laboratory Animals* (Department of Health and Human Services publication No. [NIH] 85–23, revised 1985).

Fluorescence Recording

Because conventional video imaging has not shown elevations in local $[Ca^{2+}]_i$ with depolarization of membrane patches,[13] we used laser scanning confocal microscopy and the Ca^{2+}-sensitive fluorescent indicator fluo 3 to measure $[Ca^{2+}]_i$ in an area of cytoplasm directly beneath the patch pipette. Cells were studied using a Nikon Diaphot TMD inverted microscope to which a Bio-Rad MRC-600 confocal imaging system was attached. The objective lens was a plan-apo oil-immersion lens of ×60 magnification and numerical aperture of 1.4 (Nikon). The microscope objective could be moved in the z-axis in steps of 1 μm by manual adjustment of the fine focus knob. Fluo 3 fluorescence was excited with light at 488 nm (25-mW argon-ion laser, attenuated intensity to 10%) and measured at wavelengths >515 nm. For each experiment, the recording chamber was rotated so that the long axis of the selected cell was parallel to the x-axis of the scan. Images and line scan images were obtained in all experiments with pixel dimensions of 0.271 μm and 2.60 μs, respectively. Section depth and detection volume were as described previously.[5] Computations and image analysis were carried out with a modification of an approach described previously.[7] Briefly, areas of the line scan image without elevations in $[Ca^{2+}]_i$ were selected to represent the background fluo 3 fluorescence. These areas were subtracted from the line scan image. Next, all increases in fluorescence that could be visually identified were chosen for analysis. The spatial location of the peak of the Ca^{2+} spark was defined, and a portion (30×50 pixels) of the non–background-subtracted image centered around the Ca^{2+} spark was extracted and smoothed (recursive boxcar average filter with a width of 3). The first three line scans of this area were averaged to determine the resting fluorescence. The peak amplitude of the Ca^{2+} spark was determined as the difference between the maximal fluorescence of the Ca^{2+} spark and the resting fluorescence before the peak of the Ca^{2+} spark. A threshold level was set at one-half the difference between the peak amplitude and the resting level. The rate of onset of a Ca^{2+} spark was defined as the time required for the fluorescence signal to increase from threshold to peak amplitude. The fall time of a Ca^{2+} spark was defined as the time required for the fluorescence to decrease from peak amplitude to below threshold. The following criteria were used to identify a rise in fluorescence as a Ca^{2+} spark: (1) The peak amplitude had to remain above threshold for at least two consecutive line scans (ie, 4 ms). (2) The fluorescence signal had to fall below threshold within the area analyzed. (3) The area analyzed contained only one peak of $[Ca^{2+}]_i$ elevation. $[Ca^{2+}]_i$ was calculated from the fluo 3 fluorescence with a self-ratio method using an equation and calibration parameters given previously.[4]

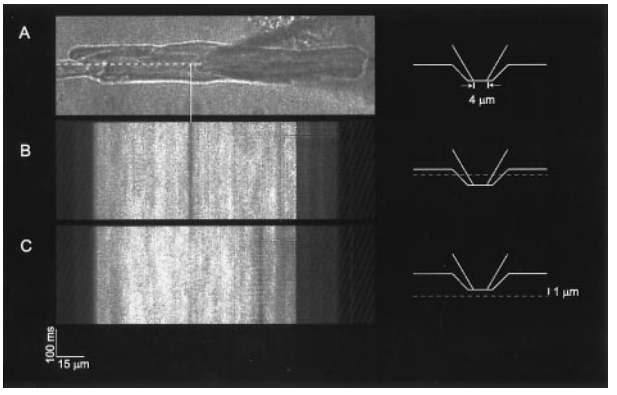

Figure 1. Localization of the scan line relative to the position of the cell-attached membrane patch. The x and y coordinates of the pipette tip (outside diameter, 4 μm) were located from the transmitted light image shown in panel A. Panels B and C show line scan images obtained by laser scanning confocal microscopy along a single line oriented parallel to the longitudinal axis of the cell through the pipette tip (dashed line). The schematic diagrams show the position of the scan line (dashed line) relative to the pipette tip. The solid vertical line shows the position of the x coordinate of the pipette tip. Differences in the depth of field of the transmitted light image (A) and the line scan images (B and C) account for the observed differences at the edges of the line scan images. The z coordinate of the pipette tip was determined by observing changes in fluo 3 fluorescence at x during changes in the focal plane (B). When the line scan intersects the pipette, the resultant image has a focal decrease in fluorescence at x, since the pipette does not contain fluo 3. For each experiment, the position of the scan line was set 1 μm below the last line scan image that showed the pipette (C).

Results

Localization of the Membrane Patch and the Line Scan Image

Since we wanted to study the relationship between Ca^{2+} entry at the membrane patch and Ca^{2+} sparks originating from the SR in direct proximity to that patch of membrane, it was necessary to localize with certainty the scan line relative to the position of the cell-attached membrane patch. As shown in Fig 1, the x and y coordinates of the pipette tip (outside diameter, 4 μm) were located from the transmitted light image (Fig 1A). The z coordinate of the pipette tip was determined by observing changes in fluo 3 fluorescence at the x position in line scan images (Fig 1A and 1B) during changes in the focal plane. When the line scan intersects the pipette, the resultant image (Fig 1B) has a focal decrease in fluorescence at x, since the pipette does not contain fluo 3. For each experiment, the position of the scan line (Fig 1C) was set 1 μm below the last line scan image that showed the pipette.

Relation of Membrane Patch Depolarization and the Occurrence of Ca^{2+} Sparks

Fig 2 shows line scan images (Fig 2A through 2C) obtained while the membrane patch was held at resting potential for 500 ms and subsequently depolarized for an additional 500 ms in a representative cell. Occasional transient nonpropagating elevations in fluo 3 fluorescence (Ca^{2+} sparks, Fig 2C) were

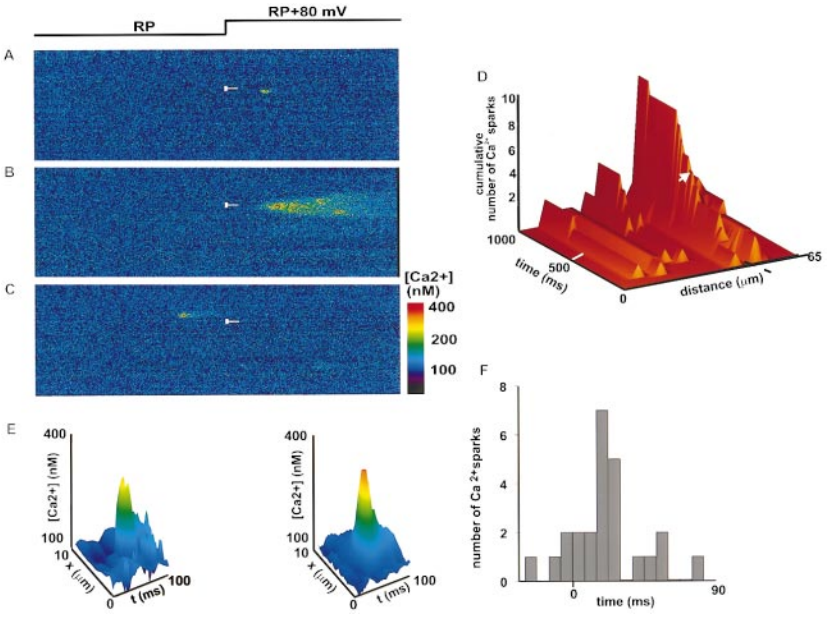

Figure 2. Relation of membrane patch depolarization and the occurrence of Ca^{2+} sparks. Line scan images (A through C) were obtained every 4 s. For each image, the membrane patch was held at resting potential (RP) for the first 500 ms and subsequently depolarized for the remaining 500 ms. The vertical scale bar represents the width of the pipette (4 μm), the horizontal scale bar represents 30 ms, and the intersection of the vertical and horizontal scale bars represents the onset of the depolarizing pulse. Depolarization of the membrane patch evoked a single Ca^{2+} spark (A), multiple Ca^{2+} sparks (B), or no Ca^{2+} sparks (C). The cumulative number of Ca^{2+} sparks at every position along the scan line from 50 consecutive membrane patch depolarizations showed an increase in the number of Ca^{2+} sparks only in the area of cytoplasm located immediately below the membrane patch (D, black dashed line). Panel E shows that the spatial and temporal characteristics of both spontaneous Ca^{2+} sparks (right; peak amplitude, 250 nmol/L; rise time, 4 ms; fall time, 28 ms) and evoked Ca^{2+} sparks (left; peak amplitude, 285 nmol/L; rise time, 4 ms; fall time, 24 ms) were similar to each other and previous reports (see text). Panel F shows the distribution of Ca^{2+} sparks with time from all 1556 scans. Bin width was 8.2 ms; note that the increase in Ca^{2+} spark rate is confined to the first 33 ms of depolarization of the membrane patch.

observed spontaneously throughout the cell both before and after depolarization of the membrane patch. In a typical cell, depolarization of the membrane patch either failed to evoke a Ca^{2+} spark (Fig 2C) or produced both single (Fig 2A) and/or multiple Ca^{2+} sparks (Fig 2B). The cumulative number of Ca^{2+} sparks at every position along the scan line from 50 consecutive line scan images from this cell is shown in Fig 2D. In response to patch depolarization, we observed an increase in the number of Ca^{2+} sparks that was confined to the volume of cytoplasm located immediately beneath the membrane patch. The spatial and temporal characteristics of both spontaneous Ca^{2+} sparks (Fig 2E, right; peak amplitude, 250 nmol/L; rise time, 4 ms; fall time, 28 ms) and Ca^{2+} sparks evoked by depolarization of the membrane patch (Fig 2E, left; peak amplitude, 285 nmol/L; rise time, 4 ms; fall time, 24 ms) were similar to each other and to previous reports.[4–9]

Also consistent with López-López et al,[5] the increase in Ca^{2+} spark rate that accompanies depolarization of the membrane patch occurs soon after the depolarization. Fig 2F presents pooled data obtained from all 1556 line scan images from 26 cells from 14 animals and shows the distribution of the occurrence of Ca^{2+} sparks directly beneath the membrane patch with time. In all 1556 line scan images, 16 Ca^{2+} sparks were observed during the first 33 ms after the onset of the depolarization and only 4 Ca^{2+} sparks were seen in the 33 ms before depolarization.

To quantify this increase in the occurrence of Ca^{2+} sparks in response to depolarization of the membrane patch, two separate analytical approaches were used. This was necessary because (1) Ca^{2+} sparks occur spontaneously,[4–8] (2) the probability of a L-type Ca^{2+} channel opening during any single depolarization is low,[7] and (3) the probability that a given L-type Ca^{2+} channel opening will trigger a Ca^{2+} spark is unknown and also probably low.[7,9] The first method assumes that Ca^{2+} sparks are independent events and calculates the probability that the observed increase in the occurrence of Ca^{2+} sparks during the depolarization could have occurred by chance. If Ca^{2+} sparks are independent events, their occurrence should be described by a binomial distribution that can be approximated by the Poisson distribution when the number of detected events is small. The total number of Ca^{2+} sparks observed in the 4-μm space beneath the patch pipette and in similar spaces located at various distances from the pipette from all line scan images (total number of line scan images, 1556) is shown in Fig 3A. The data were analyzed for 30 ms after depolarization at the pipette, since that is the time during which the maximal increase in Ca^{2+} spark rate was observed. At all other sites, the data were analyzed for 150 ms (to minimize sampling errors) and time-corrected to allow comparison with the data beneath the pipette. After depolarization, there is an increase in the occurrence of Ca^{2+} sparks only at the site of the pipette. The probability of observing this increase in the number of Ca^{2+} sparks measured beneath the pipette by chance is 0.0024.

The assumption that the Ca^{2+} sparks that occur in response to depolarization are independent of each other can be assessed by comparing the number of line scan images containing 0, 1, or more Ca^{2+} sparks with that expected from the Poisson distribution. Using the average Ca^{2+} spark rate seen ($\approx$1%), 16 sweeps were expected to have single Ca^{2+} sparks, and no sweeps were expected to have multiple Ca^{2+} sparks. Since we observed no sweeps with multiple Ca^{2+} sparks, the data support the assumption that Ca^{2+} sparks occur independently of one another in response to depolarization. This application of Poisson's theorem implicitly tests the assumption that of a great many possible Ca^{2+} sparks, only relatively few are actually observed. The implications of this finding are described below.

The second method analyzes the data with respect to the number of line scans in which Ca^{2+} sparks were observed (Fig

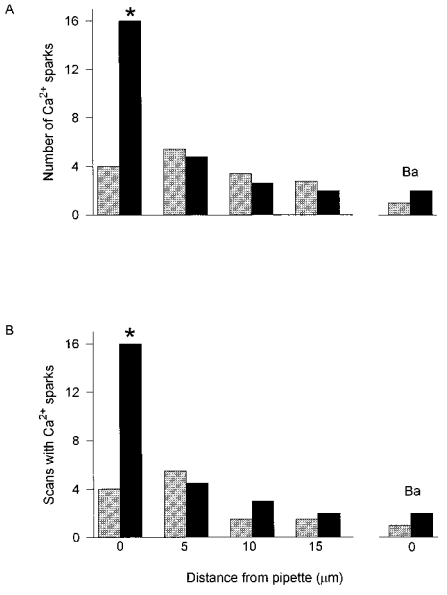

Figure 3. Statistical analyses of the occurrence of Ca^{2+} sparks in relation to depolarization of the membrane patch. Each statistical approach (A and B) represents the analysis of the pooled results obtained with either 110 mmol/L $CaCl_2$ or 10 mmol/L $CaCl_2$ as the charge carrier (total number of line scan images, 1556) and the analysis of the pooled results obtained with 10 mmol/L $BaCl_2$ as the charge carrier (total number of line scan images, 938). In panels A and B, the x-axis represents distance from the center of the pipette, the stippled bars represent Ca^{2+} sparks occurring 33 ms before depolarization of the membrane patch, and the solid bars represent Ca^{2+} sparks occurring during the first 33 ms after depolarization of the membrane patch. Ca^{2+} sparks occurring within ± 2 μm of the x position were included in the analysis. Panel A shows the total number of Ca^{2+} sparks in a 4-μm region centered at the pipette tip, and panel B shows the total number of individual line scans with Ca^{2+} sparks at each position. *$P<.01$ vs before depolarization.

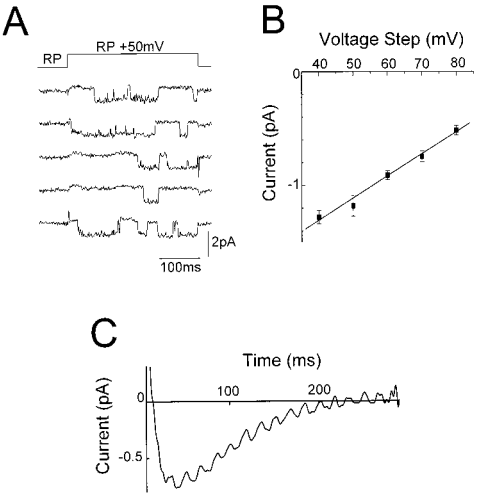

Figure 4. Single L-type Ca^{2+} channel currents in a representative membrane patch. Panel A shows representative unitary L-type Ca^{2+} channel currents from a typical membrane patch with Ba^{2+} (10 mmol/L) as the charge carrier, and panel B shows the single-channel current-voltage relation generated from the Ba^{2+} currents. RP indicates resting potential. Conductance was 19.6 pS. Panel C shows the ensemble average of L-type Ca^{2+} channel currents from 20 successive depolarizations from a large membrane patch with Ca^{2+} (10 mmol/L) as the charge carrier. There were, on average, three or four openings per sweep. A voltage step of 80 mV positive to RP generated an average inward L-type Ca^{2+} current of -0.75 pA. Ensemble-averaged L-type Ca^{2+} currents were filtered at 500 Hz, and single Ba^{2+} currents were filtered at 1 kHz.

3B). This method of analysis does not assume that Ca^{2+} sparks are independent events. Thirty-millisecond windows before and after depolarization were analyzed at each location. Once again, there is a statistically significant increase in the number of line scan images with Ca^{2+} sparks during depolarization only directly beneath the pipette (16 versus 4 images; $P=.0045$ by Fisher's exact test). When this analysis was expanded to include 150 ms before and during depolarization of the membrane patch, the probability of observing a Ca^{2+} spark was significantly increased again only in the area beneath the patch pipette ($P<.01$; data not shown). Thus, both analytical approaches demonstrate a significant increase in the probability of observing Ca^{2+} sparks directly beneath a membrane patch with depolarization.

It is apparent (Fig 3) that the presence of an on-cell patch slightly increases the probability of the occurrence of Ca^{2+} sparks in the area immediately adjacent to the pipette. This increase depends on the presence of Ca^{2+} in the pipette solution, since it is not observed when Ba^{2+} replaces Ca^{2+} as the charge carrier (Fig 3A and 3B). This probably represents the membrane effects of patch and gigaseal formation with subsequent nonspecific Ca^{2+} entry through the patch. This effect was observed with stable patches with electrical resistances of >10 GΩ. However, even with this nonspecific Ca^{2+} leak, an increase in the probability of the occurrence of Ca^{2+} sparks was still observed with depolarization of the membrane patch (Fig 3).

This increase in the probability of the occurrence of Ca^{2+} sparks with depolarization could be due to Ca^{2+} entry during the voltage step or to an independent effect of voltage.[14] However, when Ba^{2+} replaced Ca^{2+} as the charge carrier in the pipette solution, there was no increase in the probability of occurrence of Ca^{2+} sparks after depolarization at the position of the pipette (Fig 3A and 3B; total number of line scans, 938 [obtained from six cells from three animals]) or at any other sites distant from the pipette (data not shown), indicating that Ca^{2+} entry is a necessary event.

Single-Channel Currents in the Cell-Attached Membrane Patch

We have shown that there is a significant increase in the probability of the local occurrence of Ca^{2+} sparks with depolarization that is dependent on the presence of Ca^{2+} in the pipette using voltage-clamp protocols and pipette solutions designed to promote Ca^{2+} entry through L-type Ca^{2+} channels. Next, it was important to unequivocally demonstrate the presence of L-type Ca^{2+} channels under these experimental conditions. With Ba^{2+} (10 mmol/L) as the charge carrier, depolarization of a typical membrane patch (Fig 4A) resulted in frequent and prolonged openings, in this case, of at least two L-type Ca^{2+} channels (isoproterenol and Bay K 8644 were included to increase the open probability and prolong the open-time durations of L-type Ca^{2+} channels, respectively). The single-channel current-voltage relation (Fig 4B) has a conductance of 19.6 pS and is typical for L-type Ca^{2+} channels

with Ba^{2+} as the charge carrier.[15] With Ca^{2+} (10 mmol/L) as the charge carrier, single L-type Ca^{2+} channel currents could not be resolved because of their small amplitude. However, Ca^{2+} permeation in a membrane patch with several L-type Ca^{2+} channels generated an ensemble inward L-type Ca^{2+} current from 20 successive depolarizations (≈3 to 4 openings per sweep, Fig 4C) of −0.75 pA with kinetics similar to whole-cell Ca^{2+} currents obtained under identical experimental conditions.

Discussion

Since a large number of L-type Ca^{2+} channel openings occur with patch depolarization and since the application of Poisson's theorem demonstrates that relatively few of a great many possible Ca^{2+} sparks occur, we infer that only a few L-type Ca^{2+} channel openings actually trigger Ca^{2+} sparks under these experimental conditions. This suggests the need for a Ca^{2+} microdomain for efficient coupling of Ca^{2+} entry via L-type Ca^{2+} channels and SR Ca^{2+} release. This microdomain is probably disrupted under the conditions of these experiments (cell-attached patch clamp and gigaseal formation). In addition, these results provide direct experimental evidence for Ca^{2+} entry rather than voltage per se as the trigger for SR Ca^{2+} release.

Rate of Occurrence of Ca^{2+} Sparks

We estimated the rate of occurrence of Ca^{2+} sparks both at rest and with depolarization from an analysis of the line scan images and from an understanding of the optical properties of our confocal imaging system. Our strategy included the following steps: First, the volume of cytoplasm that was sampled by the line scan centered 1 μm beneath the pipette had to be determined. One dimension of this sample volume (y) corresponded to the outside diameter of the pipette (4 μm). The other two dimensions (x and z) took into account the optical characteristics of our microscope, the contribution of out-of-focus fluorescence, and the diffusion of Ca^{2+} into the sample volume from release sites distant to the scanned line. Consequently, an elevation in $[Ca^{2+}]_i$ detected in the scanned line would meet the criteria for a Ca^{2+} spark if it originated from release sites that were no more distant from the scanned line than ±0.54 μm in the x dimension and/or ±1.08 μm in the z dimension.[16] Therefore, the volume of the cytoplasm sampled by the line scan image beneath the pipette was 9×10^{-3} pL (1.08 μm×4 μm×2.16 μm). Since the line scan images were also analyzed in 4-μm segments at each of the positions indicated in Fig 3, each of these sampled areas represented the same sample volume (9×10^{-3} pL).

Having defined the sampling volume, the Ca^{2+} spark rate (r) was then calculated from the following equation:

$$r = N/(V_{total}\times T)$$

where N is the number of Ca^{2+} sparks observed in the sample volume in the 1556 line scan images, V_{total} equals the total volume sampled in the 1556 line scan images, and T is time sampled per line scan image. To determine the rate of observing Ca^{2+} sparks at rest (r_{basal}), the number of Ca^{2+} sparks observed at sites distant from the influence of the pipette (Fig 3, positions ±10 and ±15 μm from the pipette) both before and after depolarization of the membrane patch was used. Thus, r_{basal} equaled 5.93 Ca^{2+} sparks · pL^{-1} · s^{-1} or 119 Ca^{2+} sparks · $cell^{-1}$ · s^{-1} if one assumes that a typical rat ventricular cell has a volume ≈20 pL.[4] This rate is somewhat lower than the "absolute spark frequency" of 20 Ca^{2+} sparks · pL^{-1} · s^{-1} previously observed in resting rat ventricular cells[17] and may reflect differences in the estimation of the volume sampled between these studies. However, our rate is in close agreement to the Ca^{2+} spark rate of ≈100 Ca^{2+} sparks · $cell^{-1}$ · s^{-1} derived by Cheng et al[4] from a consideration of the properties and distribution of SR Ca^{2+} release channels.

From Fig 3, it is clear that there is an increase in the spontaneous Ca^{2+} spark rate in the vicinity of the pipette that is independent of the depolarization. This nonspecific increase in the Ca^{2+} spark rate was determined with the above strategy using the number of Ca^{2+} sparks observed at ±5 μm from the pipette before and after depolarization and the number of Ca^{2+} sparks observed at the pipette before depolarization. After subtraction of the basal Ca^{2+} spark rate, the nonspecific increase in the Ca^{2+} spark rate was also 119 Ca^{2+} sparks · $cell^{-1}$ · s^{-1}. Finally, using a similar analysis, the Ca^{2+} spark rate in the 30 ms after depolarization beneath the pipette was 31.5 Ca^{2+} sparks · pL^{-1} · s^{-1} or 729 Ca^{2+} sparks · $cell^{-1}$ · s^{-1}, which when corrected for the nonspecific increase due to the pipette yields 610 Ca^{2+} sparks · $cell^{-1}$ · s^{-1}. This represents a 5.1-fold increase in the Ca^{2+} spark rate in response to depolarization of the membrane patch.

This estimated Ca^{2+} spark rate is somewhat lower than might be expected intuitively from our experimental conditions and is less than the ≈6×10^3 Ca^{2+} sparks · $cell^{-1}$ · s^{-1} predicted by Cannell et al[6] on the basis of the comparison of the fractional increase in Ca^{2+} during voltage ramps (which evoked countable Ca^{2+} sparks) compared with the increase observed during normal $[Ca^{2+}]_i$ transients. A similar Ca^{2+} spark rate was suggested by Cannell et al from line scan images obtained during action potentials.[18] In spite of our efforts to minimize deformation of the membrane when forming the on-cell patch, it is likely that some alteration in the coupling between single L-type Ca^{2+} channels and the SR Ca^{2+} release channels has occurred (see "Methodical Limitations" below). Also, we cannot exclude other potential variables such as sweep-to-sweep variations in the properties of the L-type Ca^{2+} channels in the membrane patch and possible regional variations in the probability of occurrence of Ca^{2+} sparks.

Voltage-Activated SR Ca^{2+} Release

In isolated rat and guinea pig ventricular cells loaded with fura 2, Levi et al[14] have shown recently that test depolarizations to +20 mV from a holding potential of −60 mV are capable of evoking SR Ca^{2+} release under experimental conditions in which Ca^{2+} entry via L-type Ca^{2+} channels and the reverse mode of Na^+-Ca^{2+} exchange was eliminated by Ni^{2+} (5 mmol/L) and Na^+-free pipette solutions, respectively. Furthermore, this voltage-activated SR Ca^{2+} release was dependent on the presence of 100 μmol/L cAMP in the pipette solution and an experimental temperature of >30°C. However, in our experiments, we did not observe any increase in the Ca^{2+} spark rate with depolarization unless Ca^{2+} was present in the pipette. The experiments in which Ba^{2+} (10 mmol/L)

was the sole charge carrier in the pipette solution (Fig 3) strongly support the idea that the occurrence of Ca^{2+} sparks is dependent on Ca^{2+} entry rather than changes in membrane voltage per se.

Methodological Limitations

Our ability to study the relationship between single L-type Ca^{2+} channel currents and local $[Ca^{2+}]_i$ transients (Ca^{2+} sparks) depends directly on the preservation of the ultrastructural relationship between the L-type Ca^{2+} channels and the colocalized SR Ca^{2+} release channels. Because we did not directly visualize the pipette tip and the cell surface membrane after the formation of a stable gigaohm seal, we did not determine the degree to which the cell surface membrane was altered by the presence of a cell-attached membrane patch. We attempted to minimize alterations in membrane structure by using pipettes with relatively large diameters and by using little or no suction during gigaseal formation.[19] In spite of these efforts, we cannot eliminate the distinct possibility that the patch electrode closed or otherwise restricted access to an underlying T tubule. If this is indeed the case, the increased spark rate with patch depolarization shown in Fig 3 might actually represent the peripheral coupling[11] between the sarcolemmal membrane and the SR. In addition, it is also clear from Fig 3 that gigaohm seal formation and the presence of the cell-attached patch caused a nonspecific Ca^{2+} entry in the cytoplasm immediately surrounding the pipette (± 5 μm). However, this nonspecific Ca^{2+} entry increased only slightly the probability of the occurrence of Ca^{2+} sparks, and it occurred independently of the depolarization of the membrane patch.

References

1. Stern MD. Theory of excitation-contraction coupling in cardiac muscle. *Biophys J*. 1992;63:497–517.
2. Györke S, Palade P. Role of local Ca^{2+} domains in activation of Ca^{2+}-induced Ca^{2+} release in crayfish muscle fibers. *Am J Physiol*. 1993;264: C1505–C1512.
3. Sham JSK, Cleemann L, Morad M. Functional coupling of Ca^{2+} channels and ryanodine receptors in cardiac myocytes. *Proc Natl Acad Sci U S A*. 1995;92:121–125.
4. Cheng H, Lederer WJ, Cannell MB. Calcium sparks: elementary events underlying excitation-contraction coupling in heart muscle. *Science*. 1993; 262:740–744.
5. López-López JR, Shacklock PS, Balke CW, Wier WG. Local, stochastic release of Ca^{2+} in voltage-clamped rat heart cells: visualization with confocal microscopy. *J Physiol (Lond)*. 1994;480:21–29.
6. Cannell MB, Cheng H, Lederer WJ. The control of calcium release in heart muscle. *Science*. 1995;268:1045–1049.
7. López-López JR, Shacklock PS, Balke CW, Wier WG. Local calcium transients triggered by single L-type calcium channel currents in cardiac cells. *Science*. 1995;268:1042–1045.
8. Wier WG, ter Keurs HEDJ, Marban E, Gao WD, Balke CW. Ca^{2+} 'sparks' and waves in intact muscle resolved by confocal imaging. *Circ Res*. 1997; 81:462–469.
9. Shacklock PS, Wier WG, Balke CW. Local Ca^{2+} transients (Ca^{2+} sparks) originate at transverse tubules in rat heart cells. *J Physiol (Lond)*. 1995;487: 601–608.
10. Cheng H, Lederer MR, Xiao R-P, Gomez AM, Zhou Y-Y, Ziman B, Spurgeon H, Lakatta EG, Lederer WJ. Excitation-contraction coupling in heart: new insights from Ca^{2+} sparks. *Cell Calcium*. 1996;20:129–140.
11. Lewis-Carl S, Felix K, Caswell AH, Brandt NR, Ball WJ Jr, Vaghy PL, Neissnre G, Ferguson DG. Immunolocalization of sarcolemmal dihydropyridine receptor and sarcoplasmic reticular triadin and ryanodine receptor in rabbit ventricle and atrium. *J Cell Biol*. 1995;129:673–682.
12. Santana LF, Cheng H, Gómez AM, Cannell MB, Lederer WJ. Relation between the sarcolemmal Ca^{2+} current and Ca^{2+} sparks and local control theories for cardiac excitation-contraction coupling. *Circ Res*. 1996;78: 166–171.
13. Trafford AW, O'Neill SC, Eisner DA. The effects of local depolarization on $[Ca^{2+}]_i$ in isolated rat ventricular myocytes. *J Physiol (Lond)*. 1994; 477:29P. Abstract.
14. Levi AJ, Hobai IA, Dalton G, Howarth C, Pabbathi V, Hancox JC, Ferrier GR. Sarcoplasmic reticulum Ca release activated by membrane depolarization, in the absence of Ca^{2+} entry, in heart cells from rabbit, rat and guinea-pig. *Biophys J*. 1997;72:A161. Abstract.
15. Shorofsky SR, January CT. L- and T-type Ca^{2+} channels in cardiac Purkinje cells: single-channel demonstration of L-type Ca^{2+} window current. *Circ Res*. 1992;70:456–464.
16. Pratusevich VR, Balke CW. Factors shaping the confocal image of the calcium spark in cardiac muscle cells. *Biophys J*. 1996;71:2942–2957.
17. Satoh H, Blatter LA, Bers DM. Effects of $[Ca^{2+}]_i$, SR Ca^{2+} load, and rest on Ca^{2+} spark frequency in ventricular myocytes. *Am J Physiol*. 1997;272: H657–H668.
18. Cannell MB, Cheng H, Lederer WJ. Spatial non-uniformities in $[Ca^{2+}]_i$ during excitation-contraction coupling in cardiac myocytes. *Biophys J*. 1994;67:1942–1956.
19. Sakmann B, Neher E. Geometric parameters of pipettes and membrane patches. In: Sakmann B, Neher E, eds. *Single-Channel Recording*. New York, NY: Plenum Publishing Corp; 1985:37–51.